Journal Homepage
www.ajas.uoanbar.edu.iq
Anbar Journal of Agricultural Sciences
(University of Anbar – College of Agriculture)

Comparative Analysis of Quantitative and Qualitative Water Soil Erosion Assessment Methods: A Case Study of The Boudinar Watershed, Morocco

M. Taher * **I. Etebaai** **M. Lamgharbaj**
S. Ed-Dakiri **M. A. Omar** **A. Tawfik**

Laboratory for Research and Development in Applied Geosciences, Faculty of Science and Technology of Tanger, Abdelmalek Essaadi University, Tetouan, Morocco

***Correspondence to:** Morad Taher, Laboratory for Research and Development in Applied Geosciences, Faculty of Science and Technology of Tanger, Abdelmalek Essaadi University, Tetouan, Morocco.
Email: m.taher@uae.ac.ma

Article info

Received: 2025-02-19
Accepted: 2025-06-17
Published: 2025-12-31

DOI-Crossref:
10.32649/ajas.2025.159304.1657

Cite as:
Taher, M., Etebaai, I., Lamgharbaj, M., Ed-Dakiri, S., Omar, M. A., and Tawfik, A. (2025). Comparative Analysis of Quantitative and Qualitative Water Soil Erosion Assessment Methods: A Case Study of The Boudinar Watershed, Morocco. Anbar Journal of Agricultural Sciences, 23(2): 1289-1311.

Abstract

Soil erosion is a major natural hazard in the Mediterranean Rif mountainous, leading to dam siltation, land degradation, and other environmental and economic problems. The eight thematic areas selected in this study for water soil erosion mapping were rainfall, lithology, LULC, slope, soil, soil (USLE), NDVI, and temperature. The analysis of the spatial distribution of the classes within the qualifying soil erosion maps indicates that PAP/RAC is the most convincing, while EPM is the most effective for quantifying models. Field validation confirmed the accuracy and consistency of the PAP/RAC model with the observed data, reinforcing its reliability for capturing erosion processes in the Boudinar basin and highlighting areas for potential improvement in future modeling efforts. To address soil erosion in the basin, the use of the EPM model to estimate average annual soil erosion and PAP/RAC to generate a potential erosion map is recommended.

Keywords: Basin, Rif, Soil erosion, Water erosion, Soil erosion models.

دراسة مقارنة باستخدام نماذج مختلفة للقياس الكمي والنوعي لتآكل التربة: حوض بودينار أنموذجا (المغرب)

مراد الطاهر * عصام اتباعي مصطفى لمغربج سكينة الداكري
المصطفى آيت عمر عبد الحميد توفيق

كلية العلوم والتقنيات بالحسيمة، جامعة عبد المالك السعدي

***المراسلة الى:** مراد الطاهر، مختبر البحث والتنمية في علوم الأرض التطبيقية، كلية العلوم والتقنيات بالحسيمة، جامعة عبد المالك السعدي، المغرب.

البريد الالكتروني: m.taher@uae.ac.ma

الخلاصة

يُعدّ تآكل التربة أحد الأخطار الطبيعية البارزة في جبال الريف المغربي، حيث يؤدي إلى ظاهرة توحل السدود، وتدهور الأراضي خصوصا الصالحة للزراعة، إضافة إلى مشاكل بيئية واقتصادية أخرى. لذلك، تهدف هذه الدراسة إلى تحديد الخريطة الأمثل لقابلية التربة للتعرية في حوض بودينار باستعمال نماذج مختلفة. ولتحقيق هذا الهدف، تم اختيار ثماني طبقات باستخدام تقنيات التحليل الجغرافي المكاني، وهي: طبقة الأمطار، والجيولوجيا، واستخدام الأراضي والغطاء الأرضي (LULC)، والانحدار، ونوع التربة، والتربة (في نموذج USLE)، ومؤشر الغطاء النباتي NDVI، ودرجة الحرارة. تشير تحاليل التوزيع المكاني للفئات داخل خرائط التآكل النوعي إلى أن نموذج PAP/RAC هو الأكثر إقناعًا، في حين يُعتبر نموذج EPM الأكثر فعالية في النماذج الكمية. كما أكدت نتائج التحقق الميداني دقة نموذج PAP/RAC وتوافقه مع البيانات المرصودة، مما يعزز من موثوقيته في تمثيل عمليات التآكل في حوض بودينار، ويسلط الضوء على المجالات التي يمكن تحسينها في النمذجة المستقبلية. ولتقليل تآكل التربة في حوض بودينار، نوصي باستخدام نموذج EPM لتقدير الفقدان السنوي المتوسط للتربة، ونموذج PAP/RAC لإنشاء خريطة التآكل المحتمل.

كلمات مفتاحية: حوض، الريف، تآكل التربة، التعرية المائية، نماذج تآكل التربة.

Introduction

Soil erosion has a negative effect on agricultural productivity and soil fertility globally, causes dam siltation, and has adverse economic and environmental consequences (5). Geomorphological processes and anthropogenic activity are the main contributors to erosion (22) in addition to the impact of climate change and land use/land cover (LULC) patterns (33). Water-induced soil erosion is among the most significant forms of land degradation (28), due to water kinetic energy, which causes the detachment, transportation, and deposition of soil particles (17). When soil fertility diminishes due to water erosion, it has a detrimental impact on food security by undermining agricultural production (1). According to a Food and Agriculture Organization of the United Nations (FAO) report, water erosion reduces global

agrarian food production by 33.7 million tons. It is the main factor in soil degradation in Tunisia (7), 10-50 ton/ha/yr are lost in Jordan due to water erosion (21), and it affects 40% and 20% of the land area in Morocco and Algeria, respectively.

The Mediterranean countries with their semi-arid climate are threatened by soil erosion, particularly Morocco, which relies heavily on agriculture, and is considered one of the most climate-vulnerable countries in north west Africa (21 and 23). Soil erosion is more critical in the Rif region of Northern Morocco (4). Despite covering only 6% of Morocco, the region produces more than 60% of all sediments. This is due to various factors including the very small dense vegetation area (23), climate change (2), heavy and aggressive rains (23), anthropogenic pressures, and the intrinsic vulnerability of the environment (4). This causes dam siltation (12), degrades agricultural land (1, 2, 3 and 5), compromises water quality, and damages water-related structures such as canals and reservoirs (12).

Soil erosion risks in Rif catchment areas have been investigated using PAP/RAC in the watersheds of Joumouaa (21) and Arbaa Ayacha (23), USLE in Ghiss and Oued El Makhazine (4), RUSLE-USPED in Nekor (3 and 4), Fieldwork in Abdelali (4), and RUSLE-MUSLE in Tahaddart (31). However, soil erosion evaluations in the northeastern part of the Rif region have not received much attention, especially in the Boudinar basin. Therefore, this study seeks to determine the spread and severity of erosion hazards in this watershed to facilitate the formulation of conservation measures and soil management programs.

Recently, erosion has been evaluated using geographic information system (GIS) and remote sensing (RS) approaches (11), while several researchers have estimated soil erosion rates and mapped high erosion areas using different models (6). These models are classified as empirical, conceptual, and physics-based (34). This study aims to: i) identify erosion susceptibility through mapping, ii) compare the results of different quantifying and qualifying soil erosion models (AHP, PAP/RAC, EPM, and USLE), and iii) evaluate the optimal model for assessing soil erosion in the Boudinar watershed in northeastern Morocco.

This study employed the Revised Universal Soil Erosion Equation (RUSLE) and the Erosion Potential Model (EPM) to quantify soil erosion in the Boudinar basin. Additionally, the Analytical Hierarchy Process (AHP) and the Priority Actions Programme/Regional Activity Centre (PAP/RAC) framework were used to qualify and prioritize areas with high erosion risk. These four methods compare the performance of estimating the soil erosion and to map high erosion areas. Accordingly, eight thematic layers: soil, soil (USLE), lithology, land use land cover (LULC), rainfall, temperature, slope, and the Normalized Difference Vegetation Index (NDVI) were used in the current study.

Study area: The Boudinar basin, in the Driouch province, Orientale region, northeastern Morocco (Fig. 1) covers 35000 hectare (8). It is situated between latitudes 35°.22 and 34°.99 north and 3°.52 and 3°.77 west. The 40-km long Amakran river is the major waterway in the basin, flowing from the south of the study area to the north into the Mediterranean. The study area is located in mountainous regions which experience significant variability in precipitation. The area's altitude ranges from 49 to 1612 m. Over a 12-year period, annual precipitation in the basin varied from 394 to

441 mm, with a progressive decline toward the northeast (8). Agriculture is the main activity in the region though it is threatened by soil movements that reduces its productivity (29). The lithology of the watershed is composed mostly of sericite-gray-shale in the southeast and southwest and marl in the middle east. In comparison, the northern part of the basin is covered by quaternary sediments.

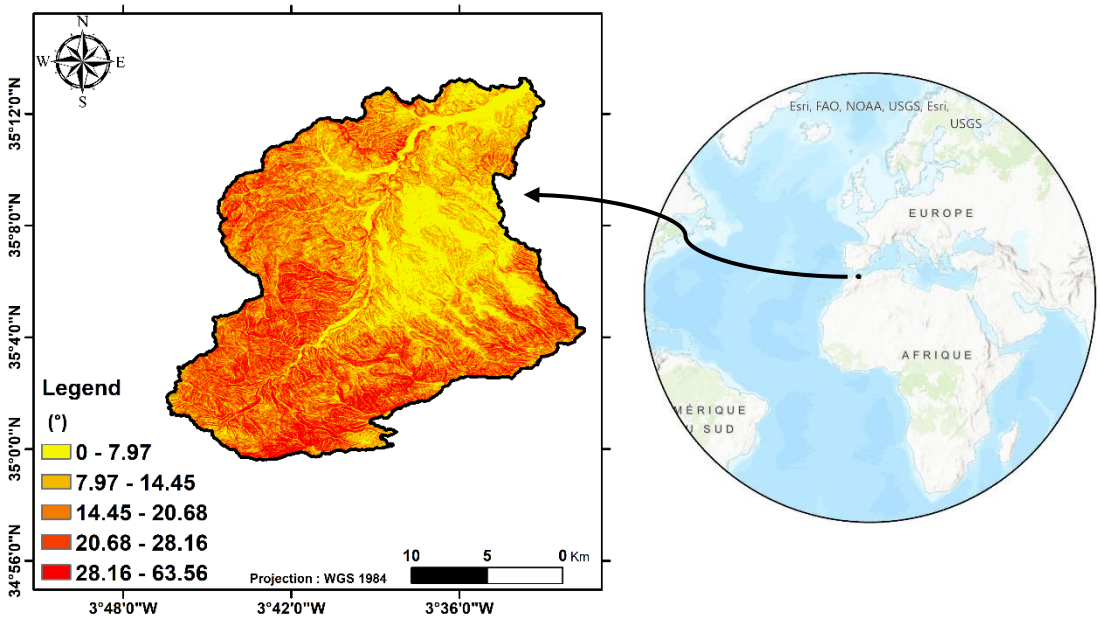

Fig. 1: The localization map of the Boudinar basin.

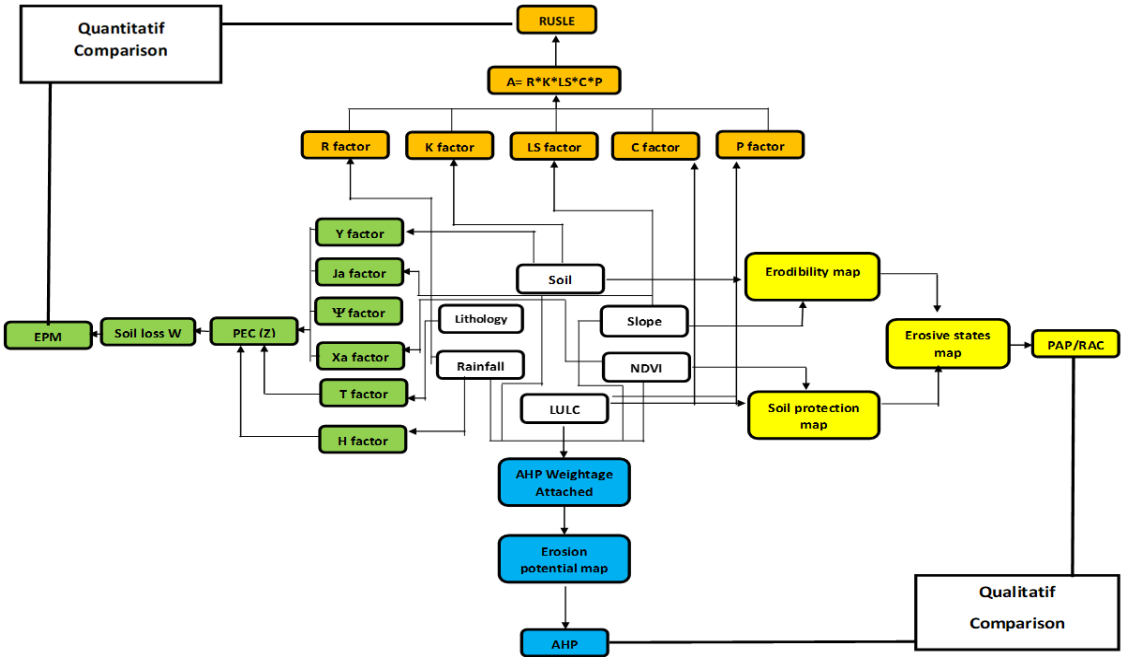

Fig. 2: Flowchart of the methodology showing the four models used in this study with the same parameters.

Materials and Methods

This study represents the first known attempt to identify and estimate soil erosion in the Boudinar basin. As a result, a key limitation is the absence of previous studies for comparison or validation of the findings. To address this, two qualitative and two quantitative models were applied. Initially, the results of each model are presented individually. This is followed by a comparison and discussion of the qualitative models (AHP and PAP/RAC) and the empirical quantitative models (EPM and USLE) (Fig. 2). Finally, the most suitable models for assessing soil erosion in the basin are identified.

Soil erosion potential parameters: The lack of local rainfall data is an important limitation of the study. However, the annual precipitation map (2010–2021) from NASA (Fig. 3b) shows rainfall in the Boudinar basin decreasing from the south to the north and ranging between 394 and 441mm. Precipitation causes the detachment, transportation, and deposition of soil particles via surface runoff. Accordingly, higher rainfall areas were more susceptible to soil erosion (high weights) than lower rainfall areas.

Both NDVI (Fig. 3a) and LULC (Fig. 3d) were the keys to soil erosion. According to the NDVI and LULC maps, the central, west, and the south of the research region have more excellent rates of vegetation (8). The NDVI value ranged between −0.06 and 0.45. Lower NDVI values were given higher weights for the potential erosion areas and vice versa (16).

The slope of a terrain contributes significantly to erosion control, as it influences the speed at which surface water runs off. Steeper slopes lead to increased runoff rates (higher weights) compared to gentler slopes. The Boudinar basin terrain exhibits varying slope gradients (Fig. 3c), ranging from 0 to 63 degrees. The northeastern and central portions of the basin predominantly feature gentle slopes, whereas steeper gradients are in the southern, southwestern, and southeastern regions (8).

Soil maps are crucial for erosion mapping as they help determine the vulnerability of soil to erosion (3). The lack of field measurements of the soil texture in the Boudinar watershed is the second significant limitation. Therefore, this study employs two kinds of soil maps. The first is for the RUSLE model. According to the FAO soil map of the world, two soil types or classes were noted in the study area, Chromic Luvisols and Calcic Cambisols (Fig. 3e). The second soil map was used for other models. The soil map of the study area revealed five different soil texture categories, spanning from fine (low weight) to coarse (high weights) texture (Fig. 3h).

Lithology is one of the essential factors for erosion. According to the lithology map (Fig. 3), three geology classes are the most vulnerable to water erosion, namely Sericite gray shale, Marl, and alluvium-silt, which covers almost the whole Boudinar basin (Fig. 3f). A high score was assigned to them. The spatial annual land temperature map (Fig. 3g) of the Boudinar watershed was obtained using 2022 Landsat 9 OLI images as the local weather stations lacked temperature data, which is the third limitation of the study. The annual average temperature ranged between 17 and 14 °C. Accordingly, regions with higher temperatures exhibited greater susceptibility to soil erosion (high

weights) compared to lower temperature areas (low weights). This factor was used only for the EPM model.

Analytical hierarchy process (AHP): The AHP method and geographic information system (GIS) have been widely used in erosion mapping (2 and 16) in Morocco (32) but not in the Rif region. The AHP uses a layer-by-layer approach to simplify complex issues, and pairwise comparisons to establish the weight of complex index systems. It was developed by Saaty (25) as the simplest of the multicriteria help methods (32). Saaty's fundamental scale in Table 1 was used to assign findings in the pairwise comparisons. The methodology adopted in this method is shown in Fig. 2.

Table 1: The Saaty scale.

Intensity	**1**	**3**	**5**	**7**	**9**
Definition (Importance)	Equal	Moderate	Strong	Very strong	Extreme

The random index scale was utilized to calculate the consistency ratio (CR) (Table 2) to test the reliability of the judgments of the computed matrix. If the CR value is less than 0.1, the consistency value for the matrix is acceptable (32). However, a value above 0.1 (10%) necessitates a reconsideration of the decision matrix (2). Therefore, in this study it was found to be quite acceptable ($0 < 0.1$). Table 3 displays the pairwise normalized matrix for calculating the parameter's weight, and Table 4 shows the sub-criteria weight of the AHP technique.

Consistency ratio (CR) = Consistency Index/Random Consistency Index (RCI)

where $CI = (\lambda max - n)/(n - 1) = (5-5)/(6-1) = 0 < 0.1$
$CR = 0$
$\lambda max = 5$

Table 2: Random Index values.

N	**1**	**2**	**3**	**4**	**5**	**6**	**7**	**8**	**9**
RI	0	0	0.58	0.89	1.12	1.25	1.32	1.40	1.45

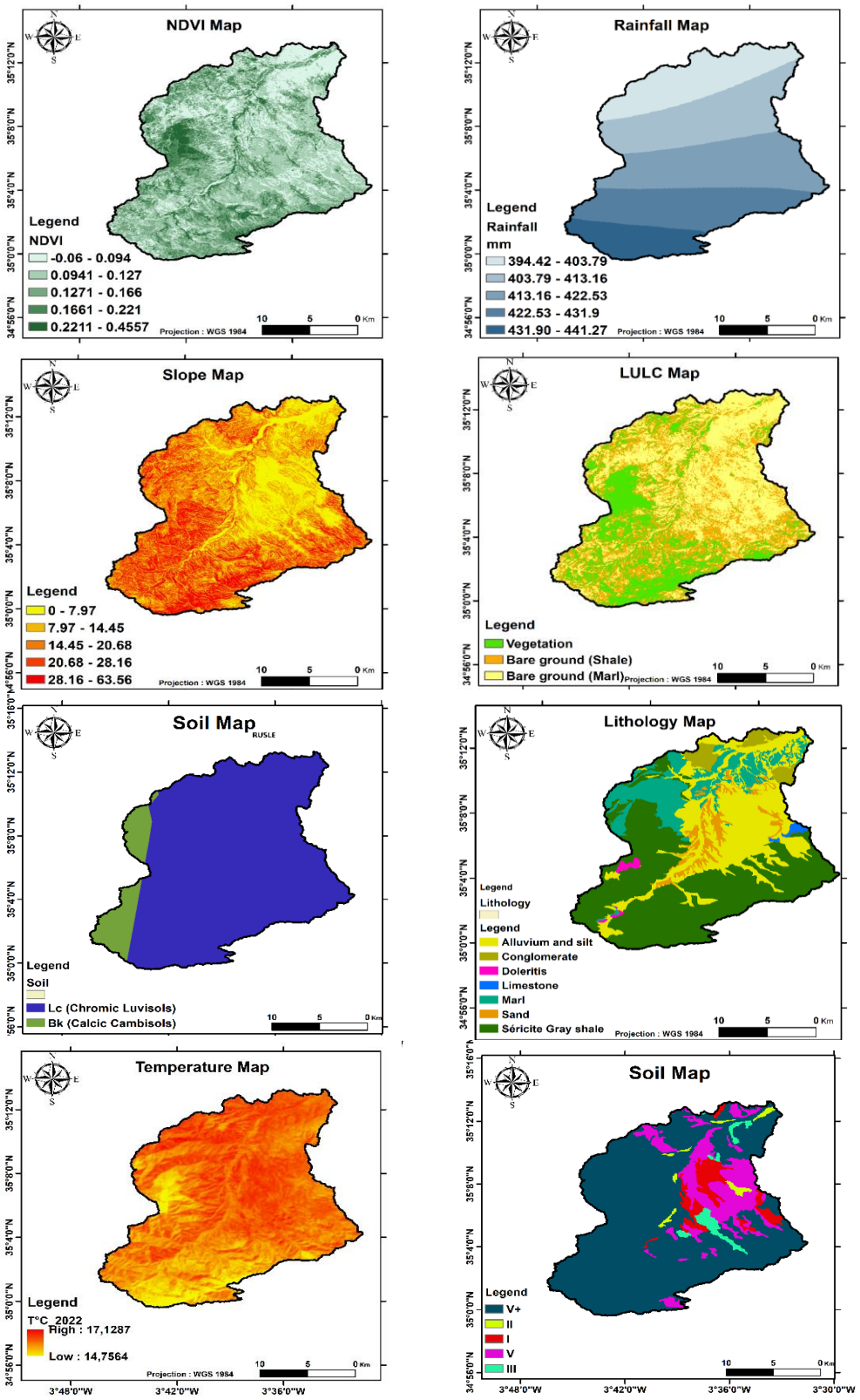

Fig. 3: Soil erosion parameters used in the methods.

Table 3: Pair-wise comparison matrix for calculating parameter weight.

Rank	**9**	**7**	**5**	**3**	**1**		
Factor	Soil	Rainfall	Slope	NDVI	LULC	CW	CW%
Soil	1	9/7	9/5	9/3	9	0.36	36
Rainfall	7/9	1	7/5	7/3	7	0.28	28
Slope	5/9	5/7	1	5/3	5	0.20	20
NDVI	3/9	3/7	3/5	1	3	0.12	12
LULC	1/9	1/7	1/5	1/3	1	0.04	4

Table 4: Normalized layer weights of the subclasses.

Influencing Factors	**Class Interval**	**Reclass**	**Overlay**	**NW%**
Soil	I	1	5	36
	II	2	4	
	III	3	3	
	V	4	2	
	V+	5	1	
Rainfall	394 – 403	1	1	28
	403 – 413	2	2	
	413 – 422	3	3	
	422 – 431	4	4	
	431 – 441	5	5	
Slope	0 – 7.	1	1	20
	7 – 14	2	2	
	14 – 20	3	3	
	20 – 28	4	4	
	28 – 63	5	5	
NDVI	-0.06 – 0.09	1	5	12
	0.094 – 0.12	2	4	
	0.12 – 0.16	3	3	
	0.16 – 0.22	4	2	
	0.22 – 0.45	5	1	
LULC	Vegetation	1	1	4
	Bare ground	2	4	

The Priority Actions Program/Regional Activity Centre (PAP/RAC): The PAP/RAC is a qualitative method of determining vulnerability to erosion and the most fragile areas (21). This is the most used method in the Rif watersheds (7, 21 and 23). This technique is part of the Mediterranean Action Plan (MAP) (7) and consists of three methodological approaches for mapping, namely predictive, descriptive, and integration (2, 7 and 27). This study only used the first approach as it does not concern erosion forms. Conversely, a qualitative comparison of sensitivity to water erosion between AHP and PAP/RAC results is achieved. The methodology adopted in this method is shown in Fig. 2.

The predictive approach thematically maps the parameters of the physical factors that control erosion, such as lithology, slope, degree of vegetation, and LULC. The three steps to achieve the predictive approach are (23):

- Producing the erodibility map by superposing the slope and soil maps.
- Generating the soil protection map by superposing vegetation density and land use.
- Developing the state of erosion map by super positioning erodibility and soil protection maps.

Erodibility map: The slope map in Fig. 3 was classified into five according to the system adopted by the PAP/RAC method (Table 5) (7 and 23). The lithology map classification (Fig. 3) had already been done by the agriculture department in the province of Nador according to the degree of soil erodibility. Thus, the erodibility map (Fig. 4) was prepared with the superposition of these two maps under the GIS environment. It shows that most of the Boudinar watershed area has high and very high erodibility.

Table 5: Classification of the input parameters of the erodibility map.

Factor	Class Interval	Reclass	Tilt
Slope	0 – 3	1	Very weak
	3 – 12	2	Weak
	12 – 20	3	Moderate
	20 – 35	4	Strong
	> 35	5	Extreme
Soil	I	1	Very weak
	II	2	Weak
	IV	3	Moderate
	V	4	Strong
	V+	5	Extreme

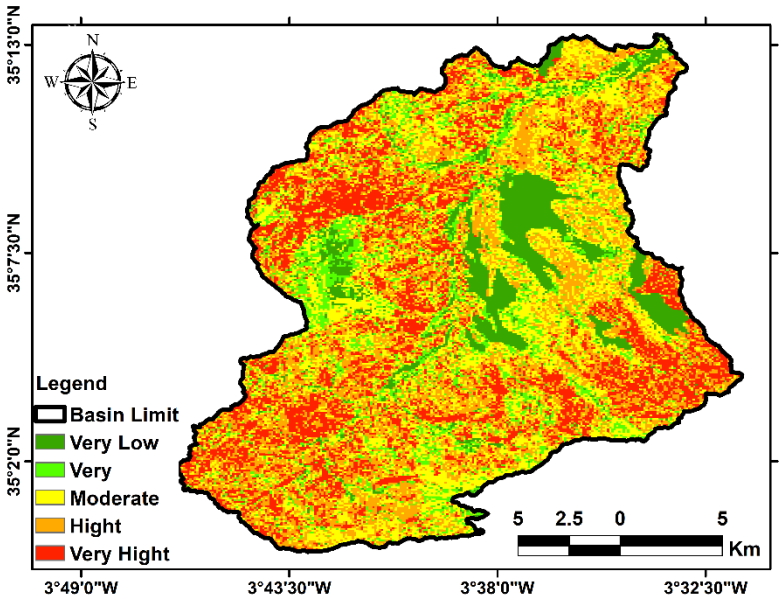

Fig. 4: Erodibility map.

Soil protection map: The NDVI map in Fig. 3 was classified into five. In the case of potential soil protection areas, greater emphasis was placed on higher NDVI values, while lower values received reduced weights (Table 6). Further, the classification of the LULC map (Fig. 3) using Landsat 9Oli image helped in identifying the two classes, i.e., the vegetation and bare ground classes, that were assigned high and low weights, respectively. Therefore, the soil protection map (Fig. 5) produced by the superposition of these two maps shows most of the Boudinar watershed area having low and deficient soil protection.

Table 6: Classification of the input parameters of the soil protection map.

Factor	Class Interval	Reclass	Tilt
NDVI	-0.06 – 0.094	1	Very weak
	0.0941 – 0.127	2	Weak
	0.1271 – 0.166	3	Moderate
	0.1661 – 0.221	4	Strong
	0.2211 – 0.4557	5	Extreme
LULC	Vegetation	4	Strong
	Bare ground	1	Very weak

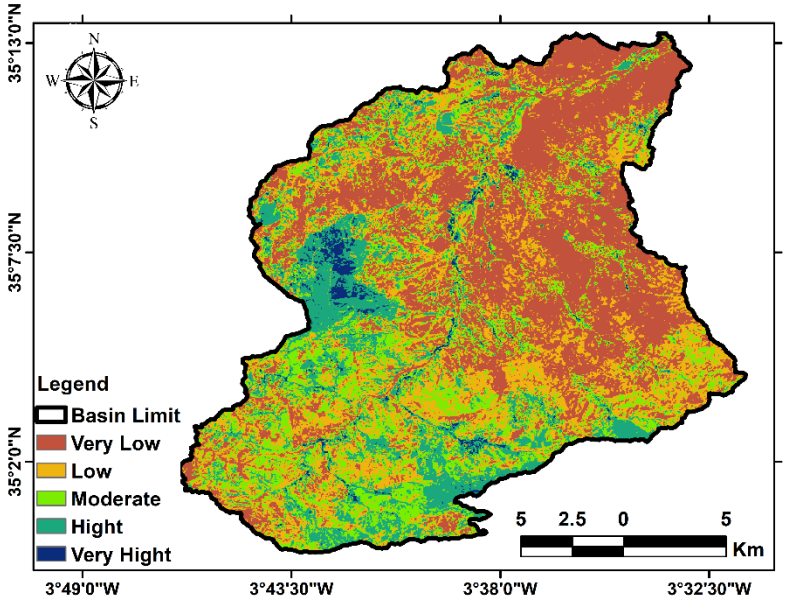

Fig. 5: Soil protection map.

Erosion Potential Model (EPM): The EPM is a quantitative method for estimating annual soil erosion rates (m3km-1y-1). It was presented for the first time in 1988 by Gavrilovic (11), and has been tested in some watersheds in Morocco (2, 11, 13 and 27), and widely used by several researchers, especially in the Balkan area, Serbia, and East-Central Europe (3, 7, 9 and 34). The thematic factors used, and the methodology adopted, is shown in Figs. 2 and 6.

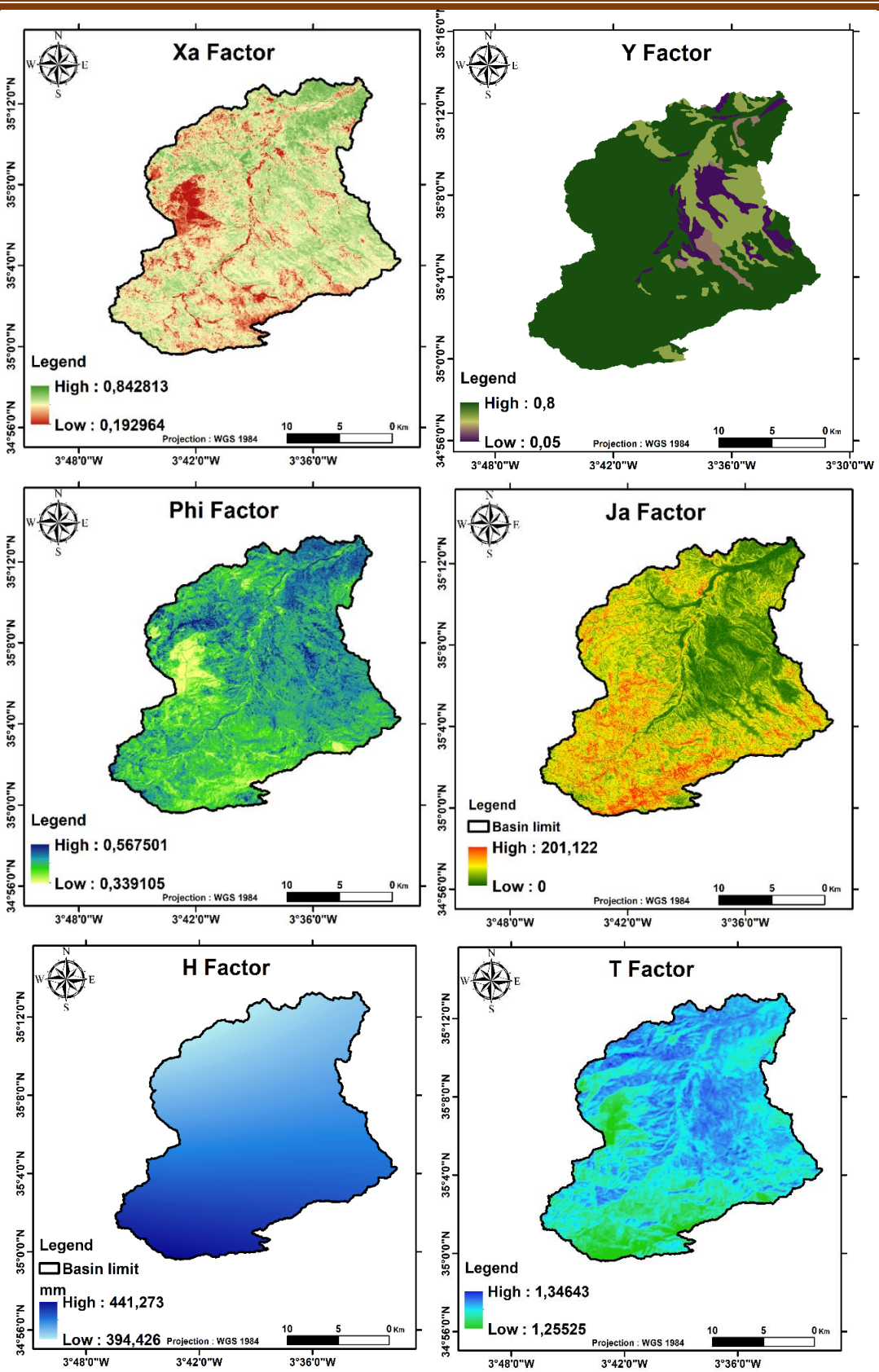

Fig. 6: The EPM factors in this study.

Universal Soil Erosion Equation (USLE): RUSLE/USLE is the second quantitative method used in this study for estimating annual soil erosion rates (t/ha/y) and has been widely used in the Rif watersheds (3, 4 and 31). It has also been used in India (1), Malaysia (1), Jordan (13), Thailand (19), as well as in Egypt (2), Nigeria (22), and

Morocco (10). The methodology and factors used in this approach are shown in Figs. 2 and 8.

The equation is expressed as: $A = R \times K \times LS \times C \times P$ (4)

where A is the annual soil erosion (t. ha-1. y-1).

The rainfall-runoff erosivity factor (R) expresses the rainfalls ability to erode soil from the surface (22). The rainfall erosive map (Fig. 8) was generated through kriging interpolation using ArcGIS software and ranges between 454 and 408. R was quantified from monthly rainfall data over 11 years (2010–2021) using Eq. (4) which was developed by Roose (1976).

$R = 0.5 \times P$ (5)

where P is the mean annual precipitation (mm).

The soil erodibility factor (K) reflects the soil's physical and chemical characteristics of texture (S), organic matter (OM) levels, structural composition, and permeability (P). The study area comprised two distinct soil types according to the FAO's world soil map. Hence, the K factor was calculated using Eq. (5):

$K = [2.1*10\text{-}4*(12\text{-}OM) *M1.14+3.25*(S–2) +2.5*(P\text{-}3)] \div 100$ (6)

where M is the product of the primary particle size fractions.

Slope length and steepness (LS) is a key factor for quantifying soil erosion and are the two topographic parameters computed from DEM (12.5×12.5 pixels) using raster calculation in ArcGIS software. The LS map (Fig. 8) was produced using the following equation:

$LS = (\text{Flow accumulation} \times \text{Cell size}/22.13)^{0.4} \times (\sin \text{Slope}/0.0896)1.3$ (7)

The LULC map (Fig. 3) is created from the Landsat 9 OLI image using the supervised classification in ArcGIS software. It was classified as vegetation and bare ground. The C factor map (Fig. 8) shows a value range of between 0.01 and 0.6. According to this map, most of the study areas have low protection against soil erosion. The area with the best protection is mostly covered by forests.

The conservation practice factor (P) is a good measure of soil management for reducing soil erosion rates (22). The P factor map (Fig. 8) was generated based on the Land Use/Land Cover map. Its values range from 0.55 to 1, with high values assigned to bare ground and minimum values to vegetation.

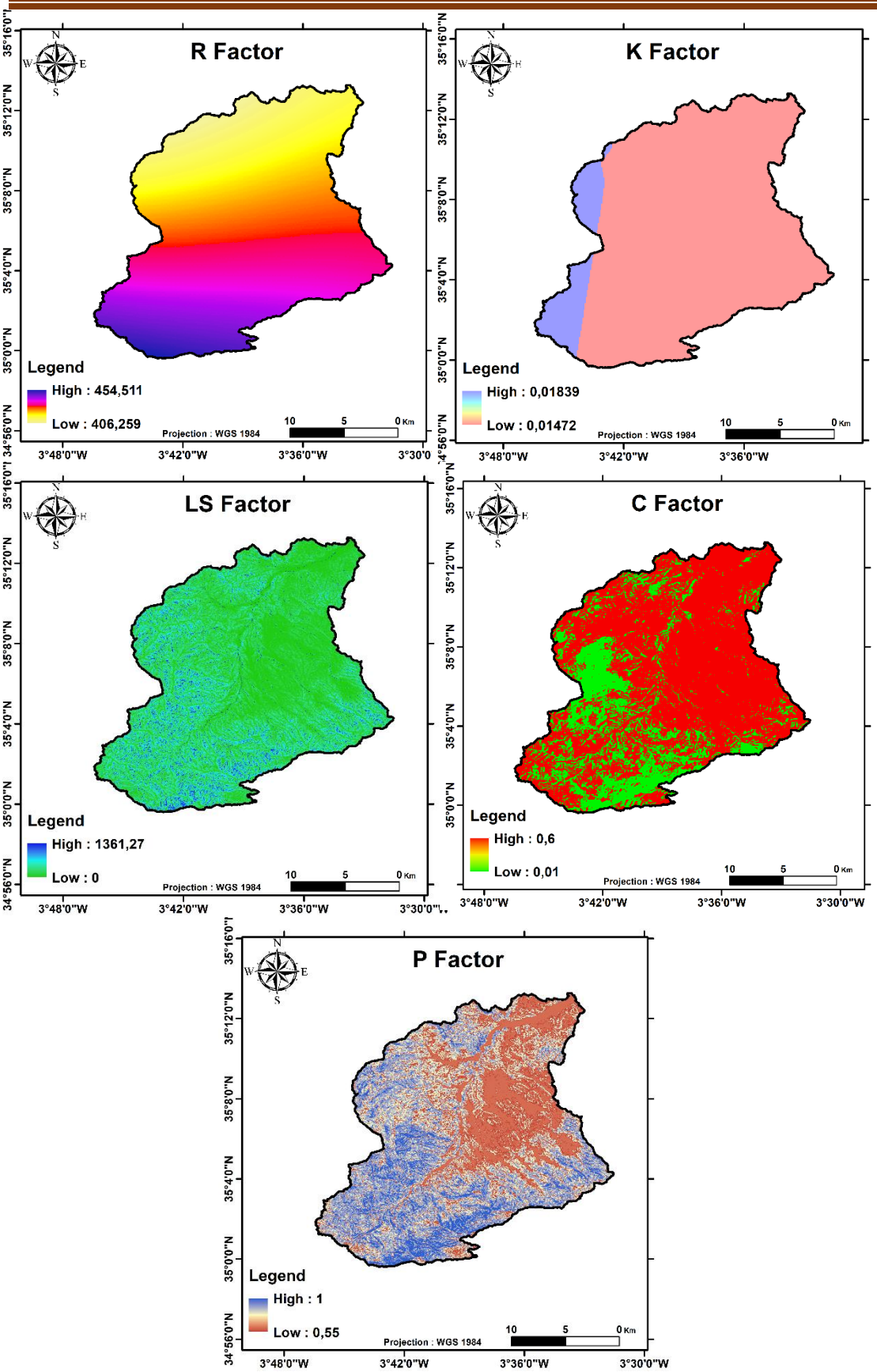

Fig. 7: The RUSLE factors used in this study.

Results and Discussion

The soil erosion risk map for the Boudinar basin using the AHP qualifying model (Fig. 9) has five classifications: very low 0.19% (comprising 0.66km^2), low 7.74% (27.09km^2), moderate 42.43% (148.50km^2), high 45.92% (160.72km^2), and very high 3.69% (12.91km^2). The method also estimated a similar proportion of high and very high erosion risk areas (48%) in the Tifnout-Askaoun basin of Southern Morocco (32). Generally, the spatial distribution of the high classes (≈50%) is concentrated in the south of the study area, whereas the low and moderate classes (≈50%) are in the north. Therefore, the soil erosion map obtained shows that the risk of erosion increases from the south to the north. The southern area of the watershed is characterized by a strong slope, heavy rainfall, and bare-fragile ground.

Based on the degree of erosivity, the map (Fig. 9) of the PAP/RAC qualifying model shows five categories: very low 9.73% (comprising 34.05 km^2), low 10.59% (37.06 km^2), moderate 28.26% (98.91 km^2), high 27.97% (97.90 km^2), and very high 23.43% (82 km^2). A similar percentage was classified as high and very high erosion risks using this method in the Arbaa Ayacha Basin, located in the western Rif region (23). The analysis of the spatial distribution of the classes' erosion map shows that the upstream of the watershed, extreme east, and the west presented high erosion risk areas (≈51%). In contrast, the low and moderate classes (≈49%) were found in the middle east of the study area, extreme middle west, and the north, which are relatively flat, have low carbonate content and very high organic matter (29). Further, the high erosion classes coincide with strong slopes, fragile lithology, low NDVI, and bare ground.

Annual soil erosion in the Boudinar watershed was estimated to be using the empirical equation of the EPM quantifying model, which showed it to be 6900 m^3/km^2/yr (≈ 69 tha^{-1}yr^{-1}.). Using the same model, erosion in the external Rif catchment was estimated at 28 t/ha/year (27), and significantly lower at 0.5 t/km²/year in the Srou Basin of the Middle Atlas (2). The annual soil erosion map (Fig. 9) rates ranged between 2.05 and 20806 m^3/km^2/yr. Similar to the USLE model, it has 6 classifications to ensure the quantifying comparison of each class. Accordingly, the very low-class forms 7.76% (27.15 km^2), low 10.06% (35.23 km^2), moderate 15.01% (52.55 km^2), high 25.9% (90.62 km^2), very high 30.4% (106.40 km^2), and extreme 10.86% (38.02 km^2). Generally, the distribution of very-low-moderate (≈33%) and high-very-extreme (≈67%) classes were similar to those of the PAP/RAC model.

The USLE is the second empirical quantifying model used in this study. The estimated average annual soil erosion in the Boudinar watershed was 20 t/ha/yr. The rates estimated in the Ghiss basin west of the study area in the same Rif mountainous region using RUSLE and USLE yielded 24 t/ha/year and 19 t/ha/year, respectively (18). Based on previous studies on erosion risk (18), the soil erosion map (Fig. 9) has six classifications: very low 55.82% (comprising 195.35 km^2), low 17.80% (62.30 km^2), moderate 10.56% (36.95 km^2), high 8.36% (29.25 km^2), very high 4.44% (15.53 km^2), and extreme 2.20% (7.66 km^2). The spatial distribution of high-very-extreme classes (15%) was almost in the same area as the other models but with lower effectiveness. Further, the very-low-moderate classes (85%) were present in most of the study area.

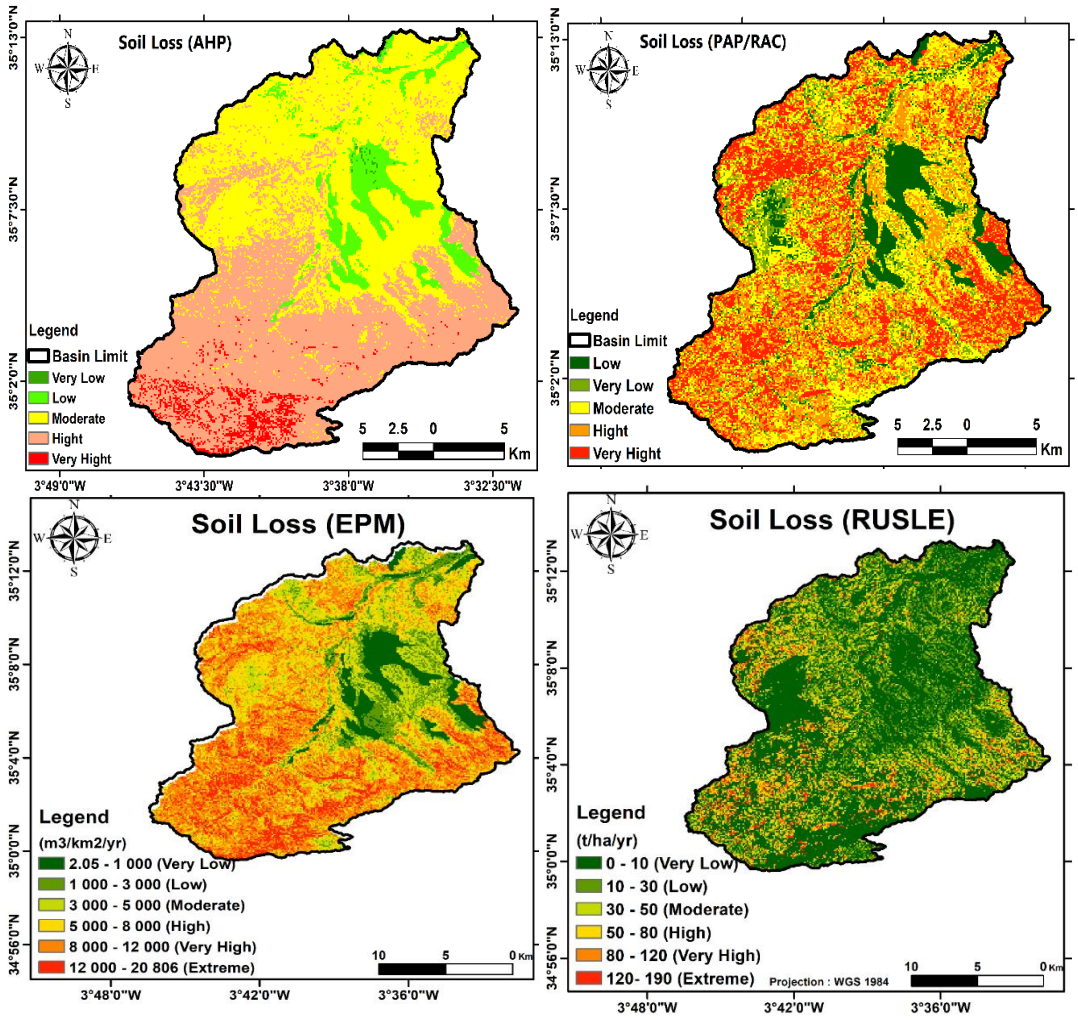

Fig. 8: Soil erosion maps of the four models used in this study.

Qualifying comparison: The rainfall factor is the main difference between the AHP and PAP/RAC models, it is an essential factor with high weightage for AHP. Hence, the concentration of the high erosion classes in the soil erosion map of AHP was in the south of the watershed, where there is heavy rainfall. In contrast, the north and the middle east of the study areas were characterized by a low risk of high erosion. This is counter to the soil erosion map of PAP/RAC model, which shows a high percentage in classification in the north and the middle east. Further, there is a significant difference in the spatial distribution of the soil erosion maps between the two qualifying models, despite the percentage similarity in the very-low-moderate and the high classes. According to Fig. 9, the high and the moderate categories dominated in the AHP soil erosion map while for the PAP/RAC model the moderate, high, and very high groups were foremost. The analysis of the geographical pattern of soil erosion in the two maps shows that the PAP/RAC qualifying model's soil erosion map is more convincing.

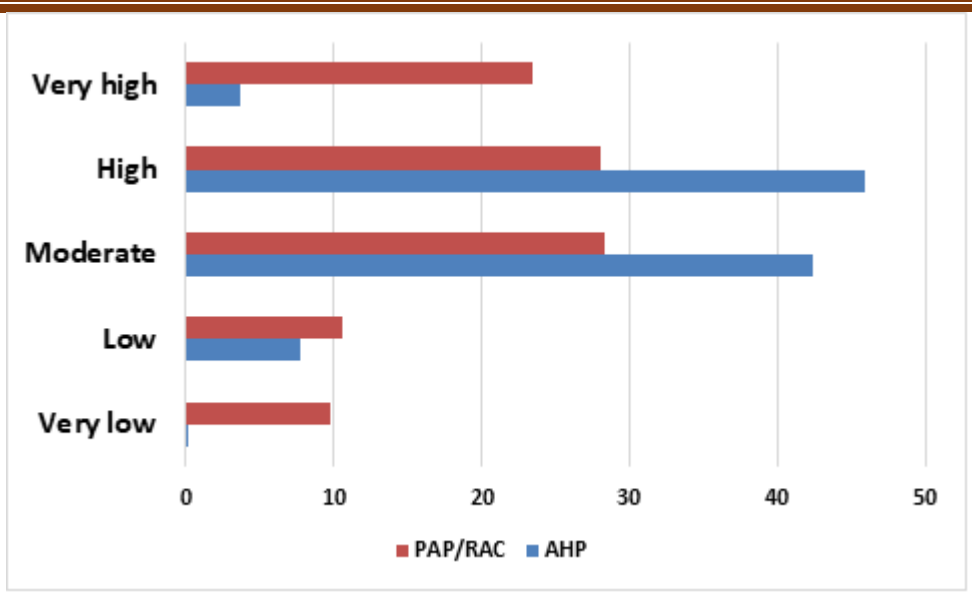

Fig. 9: Class percentage of area cover of AHP and PAP/RAC models.

Quantifying comparison: The soil thematic layer is the main limitation of the USLE model which was downloaded from the FAO soil map of the world website. Hence, it is characterized by low soil texture quality for small-scale areas as the Boudinar basin. According to this map, the basin has just two soil textures! The EPM model used the soil thematic layer of the 1:50,000 soil classification map from 1994 issued by the Nador Provincial Directorate of Agriculture; as it was based on fieldwork, it is more accurate and shows the basin having more than five soil textures. The data texture of silt, clay, and organic matter is the main reason for using the soil texture in the USLE model, to calculate the K factor. According to Fig. 10, the very-low classes were the most present in the soil erosion map of the RUSLE model, while the high-very high classes dominated in the EPM model. Therefore, despite the same spatial distribution of the erosion classes, the average annual soil erosion figures using the EPM quantifying model is much greater than the RUSLE model.

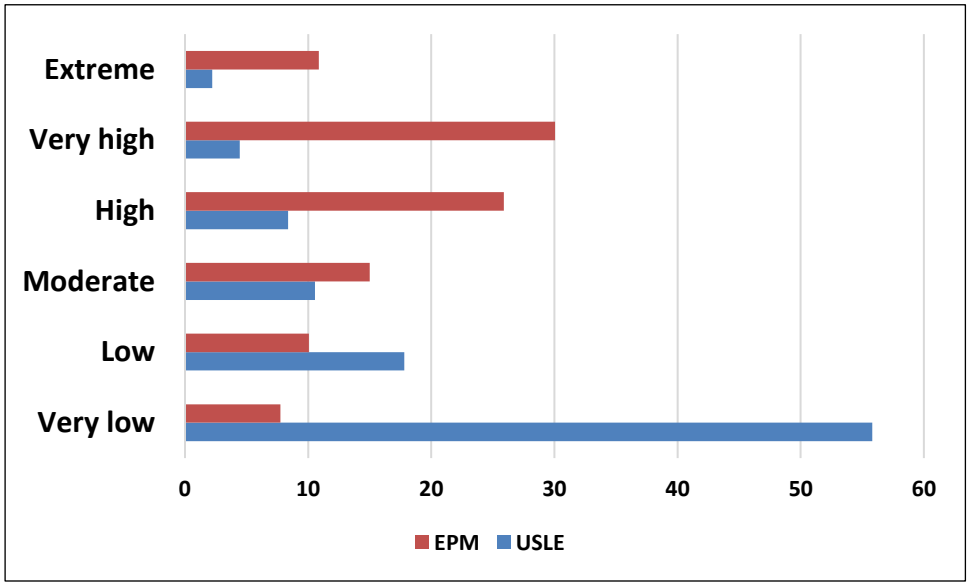

Fig. 10: Class percentage of area cover of the USLE and EPM models.

Field evaluation: Field evaluation of the obtained results is an essential step in validating any modeling. A field mission was organized to verify the accuracy of the data provided by the erosion models. Equipped with GPS devices, the mission undertook detailed mapping of erosion areas in the Boudinar basin (Fig. 11). Despite the challenges of site accessibility in certain areas, thus limiting the scope of the validation, the team was able to accurately map erosion zones in the accessible areas (see Fig. 12). Therefore, the PAP/RAC model shows agreement with the field data. This consistency reinforces confidence in the model's ability to capture erosion processes in the Boudinar basin. The field validation thus provided crucial confirmation of the erosion models studied, while highlighting challenges and potential areas for improvement for more precise modeling in the future.

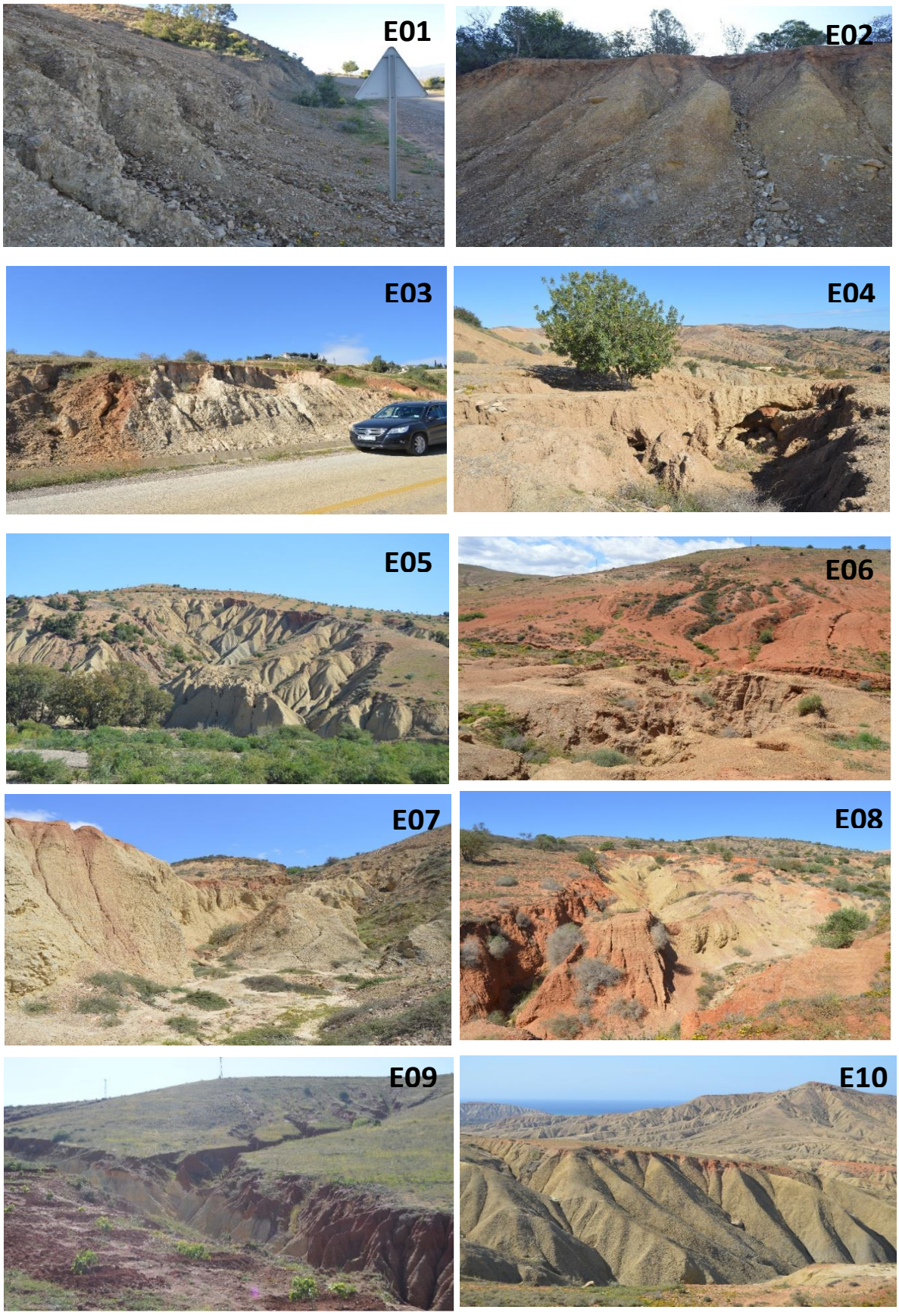

Fig. 11: Photos of the different erosion zones in the Boudinar basin.

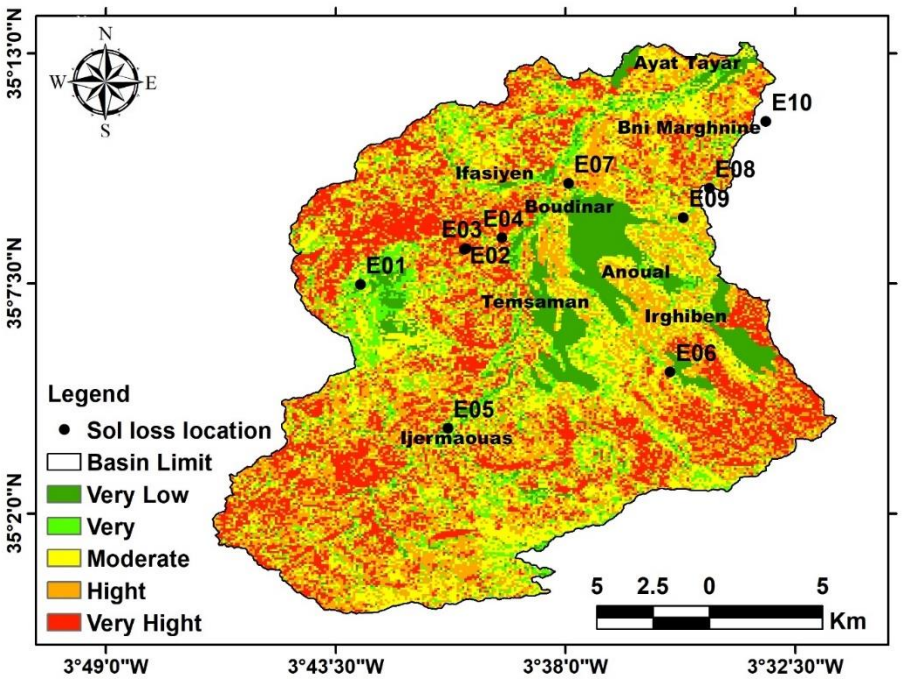

Fig. 12: Location of different erosion zones on the PAP/RAC erosion map.

Conclusions

This study presented a comparative analysis of the quantifying and qualifying factors on soil erosion in the Boudinar basin using USLE, EPM, AHP and the PAP/RAC methods. Eight thematic layers were selected and integrated into the GIS environment to produce different factors of the models used in the study. The AHP and the PAP/RAC qualifying models were first used to generate the soil erosion map. The qualifying comparison using the PAP/RAC method was found to be more effective for soil erosion mapping than the AHP method. Meanwhile, mean yearly soil erosion rates in the watershed based on EPM and USLE quantifying model calculations were 69 t/ha/yr and 20 t/ha/yr, respectively. According to the quantifying comparison between the two empirical models, the EPM model performed better in determining soil erosion rates.

Owing to the lack of field texture data, this study could not evaluate the performance of the USLE model. Hence, field work for pedologic characteristics studies was needed to produce the K factor for the model. Finally, significant similarity was noticed in the spatial distribution erosion classes between the soil erosion map of the EPM quantifying model and the PAP/RAC qualifying model. As a result, in cases where local texture data is lacking, the PAP/RAC model is recommended for generating soil erosion maps while the EPM should be used to estimate average annual soil erosion.

Supplementary Materials:

No Supplementary Materials.

Author Contributions:

Morad Taher and Issam Etebaai: methodology, writing—original draft preparation; Mustapha Lamgharbaj and Mustapha Ait Omar: field mission; Soukaina Ed-Dakiri and Abdelhamid Tawfik: writing—review and editing. All authors have read and agreed to the published version of the manuscript.

Funding:

This research received no external funding.

Institutional Review Board Statement:

The study was adhered to the protocols set out by the Ministry of Higher Education and Scientific Research, Iraq.

Informed Consent Statement:

Not applicable.

Data Availability Statement:

Data available upon request.

Conflicts of Interest:

The authors declare no conflict of interest.

Acknowledgments:

The authors are thankful for the help of the Faculty of Science and Technology of Tanger, Abdelmalek Essaadi University, Tetouan, Morocco.

References

1. Alaboz, P., Dengiz, O., Demir, S., and Şenol, H. (2021). Digital mapping of soil erodibility factors based on decision tree using geostatistical approaches in terrestrial ecosystem. Catena, 207: 105634. https://doi.org/10.1016/j.catena.2021.105634.
2. Al-Rahbi, A. K. H., Abushammala, M. F. M., and Qazi, W. A. (2020). Application of the analytic hierarchy process for management of soil erosion in Oman. International Journal of the Analytic Hierarchy Process, 12(1): 104-116. https://doi.org/10.13033/ijahp.v12i1.683.
3. Al-Taie, Sh., and Khaled, Kh. A. (2023). Land degradation assessment of soils in different land use of Southeast Nineveh Governorate. IOP Conference Series: Earth and Environmental Science, 1213(1): 012092. DOI: 10.1088/1755-1315/1213/1/012092.
4. Arrebei, N., Sabir, M., Naimi, M., Chikhaoui, M., and Raclot, D. (2020). Assessment of soil erosion with RUSLE 3D and USPED in the Nekor Watershed (Northern Morocco). Open Journal of Soil Science, 10(12): 631-642. https://dx.doi.org/10.4236/ojss.2020.1012031.
5. Belasri, A., and Lakhouili, A. (2016). Estimation of soil erosion risk using the universal soil loss equation (USLE) and geo-information technology in Oued El Makhazine Watershed, Morocco. Journal of Geographic Information System, 8(01): 98. DOI: 10.4236/jgis.2016.81010.
6. Benchettouh, A., Jebari, S., Kouri, L., and Kherchi, F. (2022). Mapping of soil erosion using the PAP/RAC directive in the Seklafa catchment, Djebel Amour region (Saharan Atlas-Algeria). Algerian Journal of Environmental Science and Technology, 8(2): 2419-2428.

7. Chokri, B. (2020). Study of Vulnerable and Water Erosion Risk Areas in Sareg Catchment (Central Tunisia) Using Remote Sensing, GIS And PAP/RAC Qualitative Approach. International Journal of Environment and Geoinformatics, 7(1): 33-44. https://doi.org/10.30897/ijegeo.623877.
8. Dai, T., Wang, L., Li, T., Qiu, P., and Wang, J. (2022). Study on the characteristics of soil erosion in the black soil area of northeast China under natural rainfall conditions: The case of Sunjiagou small watershed. Sustainability, 14(14): 8284. https://doi.org/10.3390/su14148284.
9. Dominici, R., Larosa, S., Viscomi, A., Mao, L., De Rosa, R., and Cianflone, G. (2020). Yield erosion sediment (YES): A PyQGIS plug-in for the sediments production calculation based on the erosion potential method. Geosciences, 10(8): 324. https://doi.org/10.3390/geosciences10080324.
10. El Jazouli, A., Barakat, A., Khellouk, R., Rais, J., and El Baghdadi, M. (2019). Remote sensing and GIS techniques for prediction of land use land cover change effects on soil erosion in the high basin of the Oum Er Rbia River (Morocco). Remote Sensing Applications: Society and Environment, 13: 361-374. https://doi.org/10.1016/j.rsase.2018.12.004.
11. Ennaji, N., Ouakhir, H., Halouan, S., and Abahrour, M. (2022). Assessment of soil erosion rate using the EPM model: case of Ouaoumana basin, Middle Atlas, Morocco. IOP Conference Series: Earth and Environmental Science, 1090(1): 012004. DOI: 10.1088/1755-1315/1090/1/012004.
12. Faleh, A., Navas, V., and Sadiki, A. (2005). Erosion and dam siltation in a Rif catchment (Morocco). IAHS-AISH Publlication, 2: 58 64.
13. Farhan, Y., Zregat, D., and Farhan, I. (2013). Spatial estimation of soil erosion risk using RUSLE approach, RS, and GIS techniques: a case study of Kufranja watershed, Northern Jordan. Journal of Water Resource and Protection, 5(12): 1247. http://dx.doi.org/10.4236/jwarp.2013.512134.
14. Ghanem, S. (2025). Characterization of Some Mollisols Properties in the Coastal Region (Lattakia-Syria). Journal of Life Science and Applied Research, 6(1): 9-14. DOI: 10.4103/JLSAR.JLSAR_3_25.
15. Godoi, R. D., Rodrigues, D. B., Borrelli, P., and Oliveira, P. T. S. (2021). High-resolution soil erodibility map of Brazil. Science of the Total Environment, 781 146673. https://doi.org/10.1016/j.scitotenv.2021.146673.
16. Khalid, Kh. A. (2019). Using unsupervised classification to determined land cover northren of Ninvah provianec by using Remote sensing techniques. IOP Conference Series: Journal of Physics: Conference Series, 1294(9): 092037. DOI: 10.1088/1742-6596/1294/9/092037.
17. Lahlaoi, H., Rhinane, H., Hilali, A., Lahssini, S., and Khalile, L. (2015). Potential erosion risk calculation using remote sensing and GIS in Oued El Maleh Watershed, Morocco. Journal of Geographic Information System, 7(02): 128. http://dx.doi.org/10.4236/jgis.2015.72012.
18. Lin, J., Guan, Q., Tian, J., Wang, Q., Tan, Z., Li, Z., and Wang, N. (2020). Assessing temporal trends of soil erosion and sediment redistribution in the Hexi Corridor region using the integrated RUSLE-TLSD model. Catena, 195: 104756. https://doi.org/10.1016/j.catena.2020.104756.

19. Mhaske, S. N., Pathak, K., Dash, S. S., and Nayak, D. B. (2021). Assessment and management of soil erosion in the hilltop mining dominated catchment using GIS integrated RUSLE model. Journal of Environmental Management, 294: 112987. https://doi.org/10.1016/j.jenvman.2021.112987.
20. Mosaid, H., Barakat, A., Bustillo, V., and Rais, J. (2022). Modeling and mapping of soil water erosion risks in the Srou Basin (Middle Atlas, Morocco) using the EPM Model, GIS and Magnetic Susceptibility. Journal of Landscape Ecology, 15 (1): 126-147. https://doi.org/10.2478/jlecol-2022-0007.
21. Najia, F., Bouchta, E., Mohamed, M., Benzougagh, B., and El Brahimi, M. (2021). Evaluation of water erosion by mapping and application of the PAP/RAC method in the prerif of ouazzane. Ecology, Environnement and Conservation, 12: 339-350.
22. Olorunfemi, I. E., Komolafe, A. A., Fasinmirin, J. T., Olufayo, A. A., and Akande, S. O. (2020). A GIS-based assessment of the potential soil erosion and flood hazard zones in Ekiti State, Southwestern Nigeria using integrated RUSLE and HAND models. Catena, 194: 104725. https://doi.org/10.1016/j.catena.2020.104725.
23. Ouallali, A., Moukhchane, M., Aassoumi, H., Berrad, F., and Dakir, I. (2016). The mapping of the soils' degradation state by adaptation the PAP/RAC guidelines in the watershed of Wadi Arbaa Ayacha, Western Rif, Morocco. Journal of Geoscience and Environment Protection, 4(07): 77. http://dx.doi.org/10.4236/gep.2016.47009.
24. Ostovari, Y., Ghorbani-Dashtaki, S., Bahrami, H. A., Naderi, M., and Dematte, J. A. M. (2017). Soil loss estimation using RUSLE model, GIS and remote sensing techniques: A case study from the Dembecha Watershed, Northwestern Ethiopia. Geoderma regional, 11: 28-36. https://doi.org/10.1016/j.geodrs.2017.06.003.
25. Saha, S., Gayen, A., Pourghasemi, H. R., and Tiefenbacher, J. P. (2019). Identification of soil erosion-susceptible areas using fuzzy logic and analytical hierarchy process modeling in an agricultural watershed of Burdwan district, India. Environmental Earth Sciences, 78(23): 649. https://doi.org/10.1007/s12665-019-8658-5.
26. Saaty, T. L. (1990). How to make a decision: the analytic hierarchy process. European journal of operational research, 48(1): 9-26. https://doi.org/10.1016/0377-2217(90)90057-I.
27. Senapati, U., and Das, T. K. (2022). GIS-based comparative assessment of groundwater potential zone using MIF and AHP techniques in Cooch Behar district, West Bengal. Applied Water Science, 12(3): 43. https://doi.org/10.1007/s13201-021-01509-y.
28. Stefanidis, S., and Stathis, D. (2018). Effect of climate change on soil erosion in a mountainous Mediterranean catchment (Central Pindus, Greece). Water, 10(10): 1469. https://doi.org/10.3390/w10101469.
29. Taher, M., Mourabit, T., El Talibi, H., Amine, A., Bourjila, A., Errahmouni, A., ... and Etebaai, I. (2025). Landslide Susceptibility Mapping (LSM) of the Boudinar Basin (Morocco) using the Geographic Information System (GIS) and the Analytical Hierarchy Process (AHP) method. Iranian Journal of Earth Sciences, 17(1): 1-10. https://dx.doi.org/10.57647/j.ijes.2025.1701.03.

30. Taher, M., Faraji, O., Etebaap, I., and Ghanem, S. (2025). Evaluating landslide hazard in the boudinar basin (Morocco) through soil properties. Poljoprivreda i Sumarstvo, 71(1): 129-138. https://doi:10.17707/AgricultForest.71.1.10.
31. Tahiri, M., Tabyaoui, H., Tahiri, A., El Hadi, H., El Hammichi, F., and Achab, M. (2015). Modelling soil erosion and sedimentation in the Oued Haricha sub-basin (Tahaddart watershed, Western Rif, Morocco): risk assessment. Journal of Geoscience and Environment Protection, 4(1): 107-119. http://dx.doi.org/10.4236/gep.2016.41013.
32. Tairi, A., Elmouden, A., and Aboulouafa, M. (2019). Soil erosion risk mapping using the analytical hierarchy process (AHP) and geographic information system in the tifnout-askaoun watershed, southern Morocco. European Scientific Journal, 15(30): 1857-1743. http://dx.doi.org/10.19044/esj.2019.v15n30p338.
33. Tošić, R., Lovrić, N., and Dragićević, S. (2019). Assessment of the impact of depopulation on soil erosion: case study-Republika Srpska (Bosnia and Herzegovina). Carpathian Journal of Earth and Environmental Sciences, 14(2): 505-518. http://dx.doi.org/10.26471/cjees/2019/014/099.
34. Veličković, N., Todosijević, M., and Šulić, D. (2022). Erosion Map Reliability Using a Geographic Information System (GIS) and Erosion Potential Method (EPM): A Comparison of Mapping Methods, BELGRADE Peri-Urban Area, Serbia. Land, 11(7): 1096. https://doi.org/10.3390/land11071096.